RSC Advances

PAPER

View Article Online
View Journal | View Issue

Cite this: *RSC Adv.*, 2014, **4**, 12160

MOR zeolite supported Brønsted acidic ionic liquid: an efficient and recyclable heterogeneous catalyst for ketalization

Zhang-Min Li, Yan Zhou, Duan-Jian Tao,* Wei Huang, Xiang-Shu Chen* and Zhen Yang

Received 6th January 2014
Accepted 19th February 2014

DOI: 10.1039/c4ra00092g

www.rsc.org/advances

In order to widen the application of ionic liquids as efficient and renewable heterogeneous catalysts, supported ionic liquids (SILs) have received considerable attention. A novel heterogeneous catalyst MOR zeolite supported Brønsted acidic ionic liquid (BAIL@MOR) was therefore prepared, characterized and applied in the ketalization reaction. The influences of reaction temperature, time, and catalyst loading have also been investigated in detail. Combined characterization results of XRD, FT-IR, SEM, TG-DTG and N_2 adsorption–desorption suggested that the BAIL [CPES-BSIM][HSO_4] was successfully immobilized on the surface of MOR zeolite by covalent bonds. Moreover, the catalytic performance tests demonstrated that the catalyst BAIL@MOR exhibited excellent catalytic activities in the ketalization of cyclohexanone with glycol, 1,2-propylene glycol and 1,3-butylene glycol under mild reaction conditions, as comparable with the homogeneous catalysis of the precursors [BSmim][HSO_4] and H_2SO_4. In addition, the catalyst BAIL@MOR was also found to be reusable five times without a significant loss of its catalytic activity. Thus, the heterogeneous catalyst BAIL@MOR can act as a promising candidate for the ketalization reaction.

Introduction

In recent years, ionic liquids (ILs) have received widespread attention as a new type of eco-friendly reaction medium and green solvent, owing to their particular properties such as negligible vapor pressure, wide liquid range, excellent solubility, high catalytic activity and good selectivity. ILs present broad application prospects in the field of catalysis and have been successfully used in many organic reactions such as alkylation,[1] esterification,[2] nitration,[3] acetalization,[4] ketalization[5] and so on, for which ILs obviously exhibit high catalytic activity and selectivity. The synthesis and application of ILs therefore have been concerned and reported extensively so far.

In 2002, Cole *et al.*[6] had firstly synthesized functionalized Brønsted acidic ionic liquids (BAILs) beared with an alkyl sulfonic acid and used these BAILs for the esterification of acetic acid with ethanol. On the basis of Cole's work, Gui *et al.*[7] had further illustrated the merits of using SO_3H-functionalized BAILs for esterification. Despite the excellent conversions and selectivities, several drawbacks of SO_3H-functional ILs are still restricted their further applications. For example, the high cost of functional BAILs and the homogeneous ILs catalysts tend to cause difficulties in product purification and catalyst recovery. To overcome the above-mentioned problems, there has been a surge of interest in immobilization of ILs, the so-called supported ILs (SILs), using various polymeric and inorganic support materials in order to improve their applicability in industrial catalytic processes.[8]

Generally, SILs are prepared by coating a thin layer of IL film onto and/or into the surface of desired solid support materials. Such SILs-based heterogeneous catalyst (SILC) systems not only retain the important physical and chemical features of ILs, such as nonvolatility, designability, and good thermal stability, but also possess several attractive advantages in terms of catalyst recovery, regeneration, and reuse. In 2002, Mehnert's group[9] had firstly developed a novel SILC, which was prepared by dissolving a homogeneous transition metal catalyst, [Rh(NBD)(PPh_3)$_2$][PF_6], within a multi-layer of [BMIM][PF_6] on silica gel. After that, a variety of SILCs, including mesoporous material,[10,11] carbon nanotubes,[12] magnetic nanoparticles[13,14] or polymer-immobilized[15,16] quaternary ammonium salts, phosphonium salts, and imidazolium alkyl salts, have been extensively developed for many reactions. For example, Luo *et al.*[14] had successfully synthesized novel Fe_3O_4 nanoparticle supported ILs catalyst for the one-pot synthesis of benzoxanthenes. Doherty *et al.*[16] reported peroxometalate-based polymer immobilized ionic liquids as efficient and recyclable catalyst for hydrogen peroxide-mediated oxidation.

Jiangxi Inorganic Membrane Materials Engineering Research Centre, College of Chemistry and Chemical Engineering, Jiangxi Normal University, Nanchang 330022, People's Republic of China. E-mail: djtao@jxnu.edu.cn; cxs66cn@jxnu.edu.cn; Fax: +86-791-88120843; Tel: +86-791-88121974

However, despite the excellent catalytic performance and good recyclability, most of these SILCs always showed significantly lower catalytic activity than the homologous homogeneous IL catalysts because of the lower degree of exposure of the catalytic sites.[17] In addition, the SILC systems often contain mesoporous silica, carbon nanotube and polystyrene as the supporting materials. A few examples of supported ILs can be found in the literatures where zeolite is employed as the supporting material.[18–20] Therefore, our efforts have been focused on the appropriate zeolite as support material that can effectively promote the catalytic reactivity of SILCs in comparison with the corresponding homogeneous IL catalysts.

As well known, mordenite (MOR) with a crystalline zeolite framework exhibits a higher hydrothermal stability and it is widely used as Brønsted acid catalyst for cracking, isomerisation, and alkylation reactions in the petrochemical industry, which makes MOR zeolites suitable for a potentially new supporting material.[21–23] Therefore, the introduction of SO_3H-functionalized BAILs is expected to add strong Brønsted acidity of MOR zeolite. Herein, we report a novel heterogeneous catalyst MOR zeolite supported SO_3H-functionalized BAIL (BAIL@MOR) and its application as a highly efficient and reusable catalyst in the ketalization reaction for the first time. X-ray diffraction (XRD), Fourier transform infrared (FT-IR), scanning electron microscope (SEM), thermogravimetry analysis (TG) and N_2 adsorption–desorption isotherms were then employed to characterize the catalyst BAIL@MOR in detail. Moreover, the effects of catalytic reaction parameters including temperature, catalyst loading and reaction time on the ketal yield and selectivity were explored to obtain the optimum conditions, and the reusability of the catalyst BAIL@MOR was also studied.

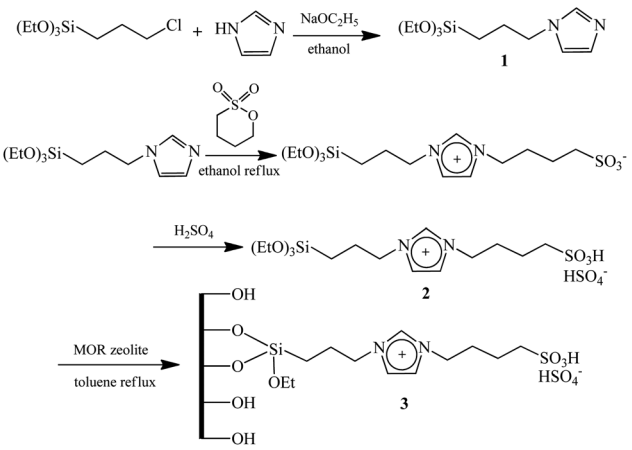

Scheme 1 General route for the synthesis of **catalyst 3** BAIL@MOR.

Experimental

Materials

3-Chloropropyltriethoxysilane (CPES, purity ≥98%), cyclopentanone (purity ≥98%), 1,3-butylene glycol (purity ≥98%) and ion-exchange resin Amberlyst 15 were purchased from Aladdin (Shanghai, China). Imidazole (purity ≥99%) and 1,4-butane sultone (purity ≥99%) were purchased from Shanghai Bangcheng Chemical Company (Shanghai, China). Commercially available mordenite zeolite powder (Si/Al ratio = 18) was purchased from Wako Pure Chemical (Code HS-642, Osaka, Japan). Other reagents such as cyclohexanone, glycol, and 1,2-propylene glycol were of analytical grade and used without any further purification.

Preparation of BAILs

The **BAIL 2** [CPES-BSIM][HSO_4] was prepared by reference to the procedure reported previously (Scheme 1).[24] In a 250 mL well-dried flask, imidazole (6.8 g) and sodium ethoxide (6.8 g) were dissolved in ethanol (100 mL), and the mixture was being stirred at 70 °C for 8 h under nitrogen atmosphere. After that, CPES (24.08 g) was added slowly over a period of 0.5 h, and the mixture was continuously refluxed for 12 h under nitrogen atmosphere. Then, the byproduct NaCl was filtered off, and the solvent ethanol was removed by rotatory evaporation. Thus the product **1** *N*-(3-propyltriethoxysilane)imidazole was obtained as a viscous liquid of light-yellow. In the second step, the synthesized precursor **1** (27.2 g), 1,4-butane sultone (13.6 g), and ethanol (100 mL) were mixed and stirred at 50 °C for 8 h. After that, sulfuric acid (9.8 g) solution in water was added slowly, and the mixture was stirred at 60 °C for 12 h to complete the reaction. The resulting solution was then washed with ether for three times and dried in vacuum at 95 °C to remove ethanol, water, and unreacted components until the weight of the residue remained constant. Therefore, the **BAIL 2** [CPES-BSIM]-[HSO_4] was obtained as a viscous liquid of yellow and its yield was near to 81%.

Preparation of BAIL@MOR

MOR zeolite was firstly pretreated in the hydrochloric acid solution (4 wt%) at 50 °C for 1 h to dissolve Al-rich amorphous materials on the surface of zeolite. At the end of hydrothermal treatment, the samples were washed repeatedly with deionized water and then dehydrated for 8 h at 80 °C under vacuum to remove physisorbed water that would be harmful to the coupling reaction.[25] For immobilization, 2.0 g of pretreated MOR zeolite was added into the previously well-mixed solution containing 1.0 g of **BAIL 2** [CPES-BSIM][HSO_4] and 100 mL of anhydrous toluene, and the mixture was refluxed at 110 °C for 24 h under nitrogen. Afterwards, the sample was filtrated and extracted with dichloromethane by Soxhlet extraction for 24 h to remove excessive **BAIL 2**. The resultant solid was then dried at 80 °C under vacuum for overnight and designated as **catalyst 3** BAIL@MOR.

Catalyst characterization

XRD patterns of samples were recorded on a Rigaku ULTIMA IV diffractometer equipped with Cu Kα radiation (λ = 1.542 Å). A continuous scan mode was used to collect 2θ from 5 to 45°, and scanning step size was 0.02° as counting time of 10 s. FT-IR spectra in the range of 400–4000 cm^{-1} were measured on a Nicolet 6700 spectrophotometer with anhydrous KBr as

standard. The particle size and morphology of samples were determined by FE-SEM (HITACHI SU8020) with an acceleration voltage of 5 kV. Nitrogen adsorption–desorption at −196 °C was measured on a BELSORP-mini II apparatus after the samples were degassed at 100 °C for 15 h under vacuum. The specific surface area was then calculated using the Brunauer–Emmett–Teller (BET) method. The TG-DTG curves were recorded on a Diamond TG/DTA thermal analyzer. Samples were heated from room temperature up to 800 °C with a heating rate of 10 °C min^{-1} under nitrogen airflow.

Catalytic test

In a typical run, the ketalization reaction was performed in a 100 mL round bottom flask with a magnetic stirrer. Weighed amounts of cyclohexanone, glycol, and catalyst (BAIL@MOR) were mixed and typically allowed to proceed for 0.5–2 h with vigorous stirring and heating at the designed temperature. After the reaction, the heterogeneous catalyst was filtered off, and then the product contained the expected ketal was detected by gas chromatography. All the samples were analyzed using HP 6890 GC analyzer (Agilent) equipped with an FID detector. A capillary column HP-1 (methyl polysiloxane, 30 m × 0.32 mm × 1 μm) was used to determine the composition of the samples with nitrogen as the carrier gas at a flow rate of about 3 mL min^{-1}. The temperatures of the column, the inlet, and the detector were kept at 180, 200, and 250 °C, respectively.

Definition of ketal yield and selectivity

The yield of ketal is defined as the ratio of the number of moles of ketal production in the reaction to the total number of moles of ketone initially added. The selectivity for ketal is defined as the ratio of the number of moles of ketal to the number of moles of ketal and other products which were detected by GC.

$$\text{Yield} = \frac{\text{moles of ketal}}{\text{moles of ketone initially added}}$$

$$\text{Selectivity} = \frac{\text{moles of ketal}}{\text{moles of (ketal + other products)}}$$

Results and discussion

Catalyst characterization

Fig. 1 displays the high-angle powder XRD patterns of MOR and BAIL@MOR. Fig. 1a shows that the XRD pattern of MOR had the typical peaks at diffraction angles of 6.51°, 9.77°, 13.45°, 22.20°, 25.63°, 26.25° and 27.67°, which was consistent well with those reported by Lu *et al.*[21] and Campbell *et al.*[26] These characteristic peaks were also present in the powder XRD patterns of **catalysts 3** BAIL@MOR, suggesting that the immobilization of **BAIL 2** on the surface of MOR zeolite did not significantly affect the skeleton of MOR zeolite (Fig. 1a and b).

The covalent binding of BAIL to the surface of MOR in **catalyst 3** BAIL@MOR was further confirmed by FT-IR spectrum

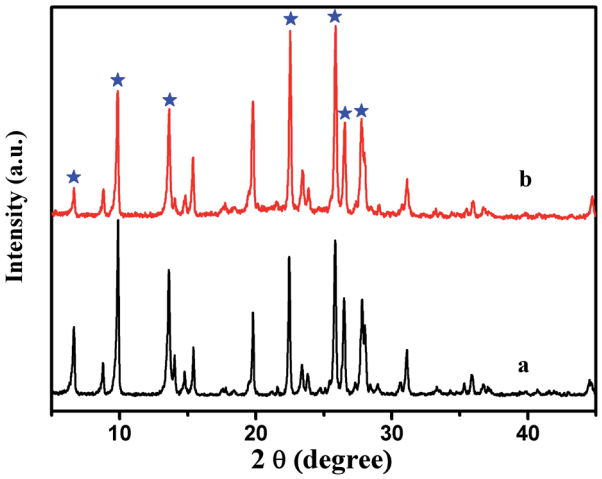

Fig. 1 Powder XRD patterns of MOR (a) and **catalyst 3** (b).

analysis. Fig. 2 gives the FT-IR spectra of **BAIL 2** and **catalyst 3**, as well as MOR zeolite for comparison. It was indicated that the FT-IR spectrum of MOR zeolite (a) had the characteristic Si–O vibrations at around 460, 812, and 1047 cm^{-1}, respectively.[10] In the hydroxyl region, the sharp band at 1630 cm^{-1} and the broad band at 3440 cm^{-1} can be attributed to a combination of the stretching vibration of Si–OH groups and the H–O–H stretching mode of adsorbed water.[14] For **BAIL 2** (c), the C–H stretching vibrations were clearly observed at 2871, 2987, and 3150 cm^{-1}, respectively. The characteristic peaks were also found at 1448 and 1586 cm^{-1}, which can be attributed to the C=C stretching vibration and the C=N stretching vibration of the imidazole ring.[27] The bands around 1039 and 1165 cm^{-1} were associated with the signals of C–S and S=O bonds, indicating the existence of $-SO_3H$ group.[28] Therefore, in comparison with MOR zeolite, the **catalyst 3** exhibited the same characteristic bands of MOR zeolite network such as the Si–O–Si vibrations (812 and 1047 cm^{-1}), the stretching vibration of Si–OH groups, and the –OH stretching vibration of adsorbed water (1630 and 3440 cm^{-1}).

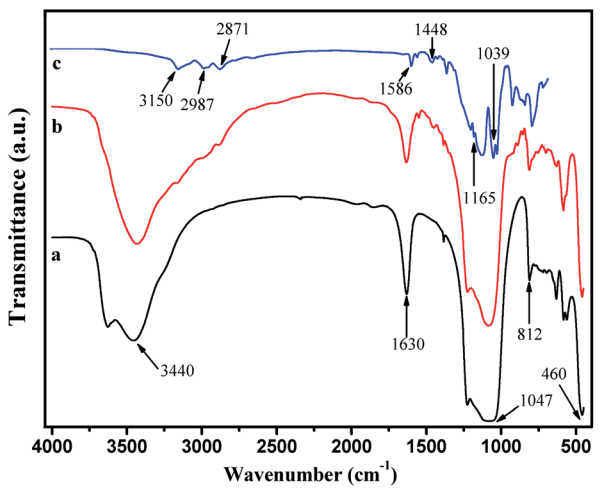

Fig. 2 FT-IR spectra of MOR (a), **catalyst 3** (b), and **BAIL 2** (c).

Moreover, it was found that the Si–OH stretching vibration of **catalyst 3** at 1630 cm^{-1} was much weaker than that of MOR zeolite, whereas the Si–O–Si vibration of **catalyst 3** at 812 cm^{-1} was stronger than that of MOR zeolite. This suggests that some of Si–OH groups on the surface of MOR were connected with BAIL obviously by the covalent binding of Si–O–Si groups. In addition, the **catalyst 3** also demonstrated newly developed C–H stretching and/or N–H stretching vibration (2871, 2987, 3150 cm^{-1}), and imidazolium ring stretching (1448, 1586 cm^{-1}). Thus, the above results indicate that the BAIL was successfully grafted onto the MOR zeolite.[14]

SEM was performed to characterize the morphology of **catalyst 3** BAIL@MOR and MOR zeolite as shown in Fig. 3. It was seen that uniform MOR zeolite was in the size of 1–2 μm (Fig. 3A). After the introduction of [CPES-BSIM][HSO_4], the size of BAIL@MOR had no obvious change (Fig. 3C), indicating that the morphological homogeneity of these MOR particles was maintained after BAIL grafting. However, the SEM images also reveals MOR particles coalescence through formation of inter-particle necks that are possibly due to the presence of the BAIL covering the MOR surfaces (Fig. 3D). In addition, at high magnifications, it was observed that the surface of MOR was rough, whereas the surface of BAIL@MOR was much plain (Fig. 3B and D). This finding demonstrated that the surface of MOR had been coated with BAIL [CPES-BSIM][HSO_4] successfully, forming a compact and thin surface layer.

Furthermore, thermal analysis was performed to monitor the decomposition profiles of MOR, **BAIL 2**, and **catalyst 3** (Fig. 4). The TG curve of the bare MOR support presents a minor weight loss in the range of 50–120 °C, which is attributed to the release of physisorbed water (Fig. 4a). As for **BAIL 2**, a significant weight loss, contributing nearly 80 wt% of the sample, was seen in the temperature range from 100 °C to 700 °C (Fig. 4c). In comparison with MOR support and **BAIL 2**, the **catalyst 3** BAIL@MOR showed three distinct steps of weight losses in the combined TG-DTG curves upon heating from room temperature to 700 °C under airflow (Fig. 4b). The first weight loss at 90 °C was due to the removal of surface-adsorbed water.[29] The second weight loss at 210 °C was probably due to the loss of surface silanol groups and structural water within MOR zeolite. The third weight loss at 250–380 °C was assigned to the successive decomposition of the imidazolium-functionalized trialkoxysilane moiety and alkyl sulfonic acid group.[24] Thus, it was demonstrated that the **catalyst 3** exhibited good thermal stability onward 160 °C and the residual weight was about 75% around 700 °C. On the basis of these results, it can be concluded that most **BAIL 2** [CPES-BSIM][HSO_4] have been well loaded on the MOR zeolite support. This is also indirect evidence of the success of immobilization of BAIL on MOR zeolite.

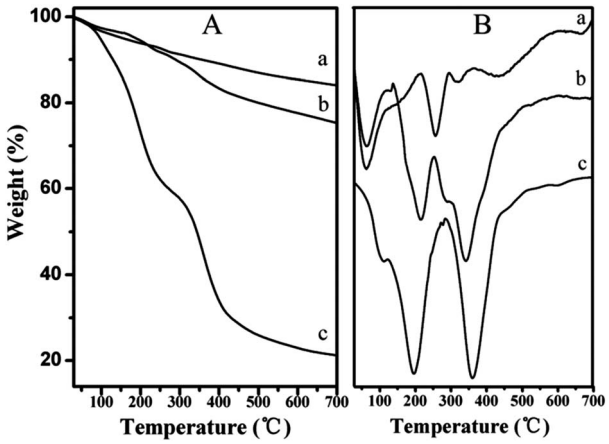

Fig. 4 Thermogravimetric (A) and differential thermogravimetric (B) results of MOR (a), catalyst 3 (b), and BAIL 2 (c).

Fig. 5 shows the N_2 adsorption–desorption isotherms of MOR zeolite and **catalyst 3** BAIL@MOR. It was clearly that all the samples exhibit type-I curves at p/p_0 = 0.0–1.0, which is characteristic of a microporous structure.[21] From the BET

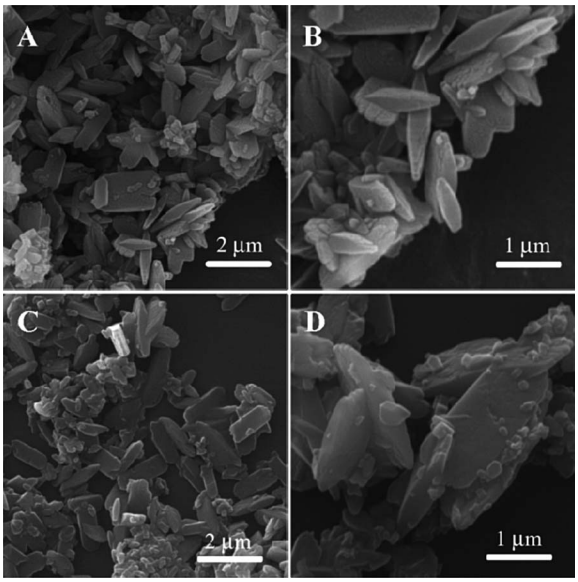

Fig. 3 The whole and magnified SEM images of MOR (A and B), and catalyst 3 (C and D).

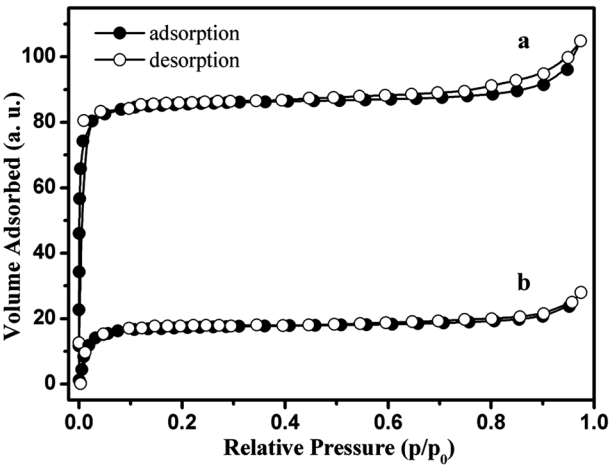

Fig. 5 N_2 adsorption–desorption isotherms of MOR zeolite (a) and catalyst 3 (b).

surface area analysis, the **catalyst 3** was found to have relatively lower BET surface areas compared with MOR zeolite. For example, MOR zeolite showed the BET surface area of 339 $m^2 g^{-1}$, whereas the BET surface area of **catalyst 3** was only 71 $m^2 g^{-1}$. The decreases in the BET surface areas of **catalyst 3** were attributed to the immobilization of BAIL onto the framework of MOR zeolite, resulting in the block of micropores and the decrease of surface areas. This finding further revealed that the BAIL had been successfully grafted onto the framework of MOR zeolite. Similar results had also been reported previously by Liu *et al.*[30]

Catalytic performance of BAIL@MOR

[BSmim][HSO_4] and MOR zeolite support were employed as catalysts for the ketalization reaction of cyclohexanone with glycol to assess their catalytic activities, and then the results were listed in Table 1. It was obvious that MOR zeolite catalyzed the reaction to have conversion of 27.9% at 2 h, showing that the support material MOR zeolite has relatively poor catalytic activity (entry 1). In sharp contrast, with the successful immobilization of **BAIL 2** onto the MOR support, the **catalyst 3** gives a drastic increase in the catalytic activity and the conversion of cyclohexanone at 2 h was nearly 70%, as comparable with the corresponding homogeneous catalysis of [BSmim][HSO_4] under the identical reaction conditions (entries 2 and 3). It is mainly due to the cooperation of Brønsted acid site from BAILs and MOR zeolite.[20] Besides, the BAILs was supported on the out surface of MOR zeolite which was microporous structure. This finding illustrated that MOR support plays a catalytic role on the ketalization reaction, and the heterogeneous catalysis of **catalyst 3** can remain high catalytic performance, even though the nominal weight of the immobilized BAIL over BAIL@MOR was significantly less than the pure BAIL.

For comparison, the ketalization of cyclohexanone was also studied without catalyst or in the presence of two conventional catalysts. As it has been found, in the absence of a catalyst, the cyclohexene conversion was very low, showing that the ketalization reaction was very difficult to occur without catalyst (entry 4). In addition, it was also showed that the conversion of cyclohexanone in the presence of the resin Amberlyst 15 and H_2SO_4 was 60.6% and 70.6% at 2 h, respectively (entries 5 and 6). This finding demonstrated that the heterogeneous catalysis of **catalyst 3** plays the equal catalytic performance in comparison with the homogeneous catalysis of H_2SO_4, showing BAIL@MOR could be used as efficient heterogeneous SILs catalysts in the ketalization reaction.

Table 1 Ketalization of cyclohexanone with glycol under various reaction systems[a]

Entry	Catalyst	The conversion of cyclohexanone[b] (%) 0.5 h	2 h	TOF[c] (h^{-1})
1	MOR	19.5	27.9	—
2	BAIL@MOR	62.9	69.5	1835
3	[BSmim][HSO_4]	67.7	71.3	230
4	Blank	0.9	3.8	—
5	Amberlyst 15	50.6	60.6	—
6	H_2SO_4	67.0	70.6	71

[a] Cyclohexanone (50 mmol), glycol (50 mmol), catalyst (0.5 wt%, based on the mass of cyclohexanone), reaction temperature (50 °C). [b] The conversion of cyclohexanone was achieved by GC analysis, and no byproducts were found by GC. [c] TOF defined as mol(ketalization) per mol(SO_3H) per h (full reaction time).

Effects of reaction parameters

Since the **catalyst 3** BAIL@MOR showed good catalytic activity, the effects of reaction parameters such as temperature, reaction time and catalyst loading were examined in detail. First, the ketalization reaction of cyclohexanone was performed in the presence of **catalyst 3** BAIL@MOR at 30 °C, 40 °C, 50 °C, and 60 °C, with cyclohexanone to glycol molar ratio of 1 : 1, and catalyst loading of 0.5 wt% (based on the mass of cyclohexanone). Fig. 6 shows the effect of reaction temperature on the conversion of cyclohexanone. It was indicated that the conversion of cyclohexanone increased rapidly with the increase in the reaction temperature. For example, the conversion of cyclohexanone at 2 h increased obviously from 58% to 70% with the rise of temperature from 30 °C to 50 °C. However, a slight increase in the conversion of cyclohexanone at 2 h was observed while the temperature was increased from 50 °C to 60 °C. This result suggests that an optimized reaction temperature should choose at 50 °C to reach the considerable catalytic activity.

The effect of different catalyst loadings on the conversion of cyclohexanone was studied by varying the catalyst loading from 0.1 wt% to 1 wt% at a temperature of 50 °C and with cyclohexanone to glycol molar ratio of 1 : 1. The results as shown in Fig. 7 indicated that, with an increase in the relative amount of catalyst, the rate of ketalization reaction was enhanced, resulting in a higher reaction rate for the conversion of cyclohexanone. For example, the conversion of cyclohexanone increased from 60% to 70% with the increase in the amount of **catalyst 3**

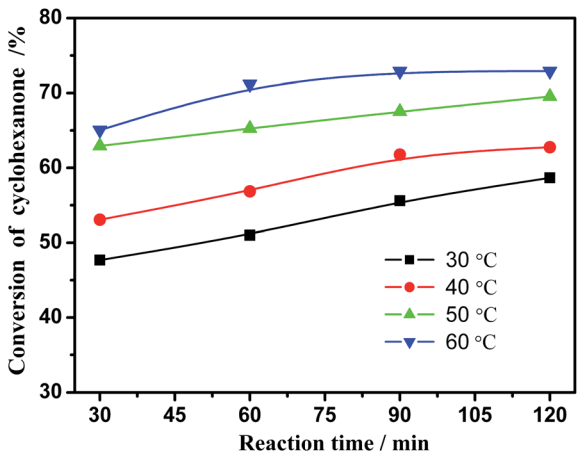

Fig. 6 Effect of temperature on the conversion of cyclohexanone with time using catalyst 3.

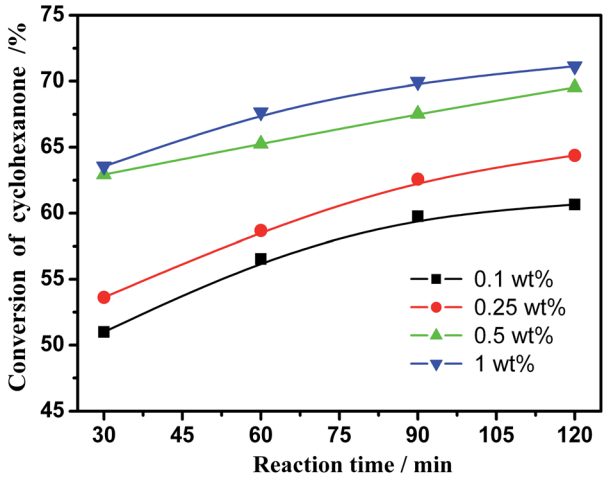

Fig. 7 Effect of catalyst loading on the conversion of cyclohexanone with time using **catalyst 3**.

from 0.1 wt% to 0.5 wt%. However, only a fair change was obtained in the conversion of cyclohexanone when the amount of catalyst was increased 2 fold from 0.5 wt% to 1.0 wt%. Beyond a certain catalyst loading, the conversion of cyclohexanone was improved slightly with increasing of catalyst loading. This implies that the further increase in the amount of catalyst is not very necessary for the conversion of reactants. Considering the reaction rate and the cost of catalyst, 0.5 wt% is taken as the optimum catalyst loading and used in most of the ketalization experiments.

In order to investigate the scope on **catalyst 3** BAIL@MOR in the synthesis of other ketals, the ketalization reactions of ketones with different diols were also tested under the optimal condition. The results were summarized in Table 2. It was demonstrated that the **catalyst 3** performed high catalytic performances in the ketalization reaction of cyclohexanone with glycol, 1,2-propylene glycol and 1,3-butylene glycol, affording the corresponding ketals in excellent yields (entries 1–3). Compared with the other two diols, 1,2-propylene glycol possessing an electron-donating methyl group resulted in the highest yield of corresponding ketal (80%), showing that the methyl group is beneficial to the nucleophilic ability of 1,2-propylene glycol and thus the yield of ketal. Future, it was also found that the yields were too low in the ketalization of cyclopentanone with the three diols (entries 4–6). The similar results were also obtained by Qi *et al.*[31] This fact was attributed to the relative reactivity and stability of cyclohexanone with six-membered ring in comparison to cyclopentanone with five-membered ring. Furthermore, we compared the catalytic performance of **catalyst 3** with the results of other heterogeneous catalysts which published in the literatures (entries 7–10).[32–35] It was found that a large excess of diol was often taken to improve the performance of those heterogeneous catalysts, and a dehydrative agent for removing the water generated in the ketalization reaction must be also required to achieve considerable yield. By contrast, without the aid of dehydrative agent and much more diol, the **catalyst 3** also displays the comparable catalytic performance in comparison with H_2SO_4 and those heterogeneous catalysts under mild conditions, indicating that BAIL@MOR can act as an efficient heterogeneous catalyst for the ketalization reaction.

Recycling of catalyst

The recycling capability is of importance for the evaluation of a heterogeneous catalyst. Thus, a series of repetitive experiments had been conducted to test the reusability of **catalyst 3** BAIL@MOR and reproducibility of catalytic performance (temperatures of 50 °C, cyclohexanone to glycol molar ratio of 1 : 1, catalyst loading of 0.5 wt%, and reaction time of 0.5 h and 2 h). In each cycle, the **catalyst 3** was separated from the reaction mixture by filtration and then washed with dichloromethane, followed by drying before the next run. The conversions of cyclohexanone from five consecutive runs thus were as shown in Fig. 8. The results demonstrated that **catalyst 3** can be recycled for up to five times with no appreciable decrease in the conversion of cyclohexanone, which demonstrates that the prepared **catalyst 3** possesses excellent stability and reusability. The slight decrease in conversions should be probably because the slight loss of partial **catalyst 3** along the continuous separation process.

Table 2 Ketalization of different ketones with diols

Entry	Catalyst	Ketones	Diols	Molar ratio	Catalyst dosage	Reaction conditions	Yield/ %	Sel./ %	Ref.
1	BAIL@MOR	Cyclohexanone	Glycol	1 : 1	0.245 g	50 °C, 2 h	69.5	100	This
2			1,2-Propylene glycol				80.1	100	study
3			1,3-Butylene glycol				68.1	100	
4		Cyclopentanone	Glycol				28.3	100	
5			1,2-Propylene glycol				39.4	100	
6			1,3-Butylene glycol				40.0	100	
7	HY zeolite	Cyclohexanone	Catechol	1 : 1	0.25 g	Reflux temperature, cyclohexane 10 mL, 4 h	80.7	99.7	32
8	Amorphous tin(IV) phosphate	Cyclohexanone	Glycol	1 : 1.3	1/65 mole of ketone	Dean–Stark conditions, 3 h	91	—	33
9	Bismuth subnitrate	Cyclohexanone	Glycol	1 : 1.5	0.25 g	82 °C, cyclohexane 15 mL, 0.5 h	94.5	—	34
10	HMCM-22	Cyclohexanone	Glycol	1 : 1.2	0.2 g	Dean–Stark conditions, 2 h	98.5	100	35

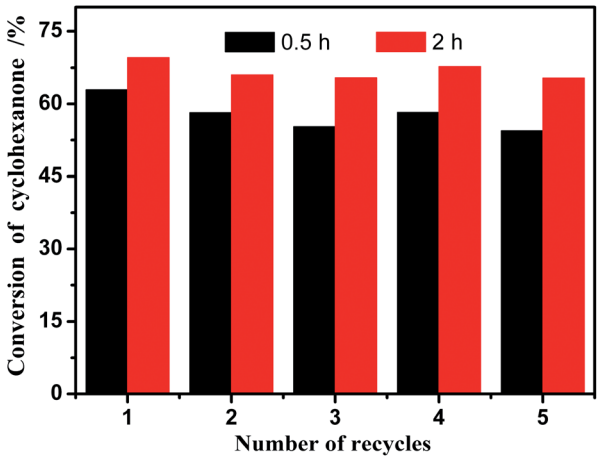

Fig. 8 The recycle test of catalyst 3 in the ketalization reaction of cyclohexanone with glycol.

Conclusions

In this study, a novel heterogeneous catalyst BAIL@MOR was successfully prepared, characterized and applied in the ketalization reaction. On the basis of characterization results, the BAIL [CPES-BSIM][HSO_4] was proved to be immobilized successfully onto MOR zeolite. Moreover, the catalytic performance tests demonstrated that BAIL@MOR played excellently catalytic performances in the ketalization of cyclohexanone with glycol, 1,2-propylene glycol and 1,3-butylene glycol, as comparable with the homogeneous catalysis of the precursors [BSmim][HSO_4] and H_2SO_4. The conversion of cyclohexanone was also found to improve effectively by increasing the reaction temperature and catalyst loading in the presence of BAIL@MOR as catalyst. In addition, the recycling tests showed that BAIL@MOR could be reused for five times without a significant loss of its catalytic activity. The heterogeneous catalyst BAIL@MOR therefore can act as an efficient and promising candidate for the ketalization reaction.

Acknowledgements

The authors are grateful for the financial support of this study from the National Natural Science Foundations of China (no. 21206063), and the Science & Technology Supporting Programs and the International Technological Cooperation Programs of Jiangxi Provincial Department of Science and Technology (no. 20123BBE50081 and 20132BDH80003).

Notes and references

1 L. Crowhurst, N. L. Lancaster, J. M. P. Arlandis and T. Welton, *J. Am. Chem. Soc.*, 2004, **126**, 11549–11555.
2 Y. Q. Deng, F. Shi, J. J. Beng and K. Qiao, *J. Mol. Catal. A: Chem.*, 2001, **165**, 33–36.
3 N. L. Lancaster and V. Llopis-Mestre, *Chem. Commun.*, 2003, 2812–2813.
4 Y. Wang, X. Gong, Z. Wang and L. Dai, *J. Mol. Catal. A: Chem.*, 2010, **322**, 7–16.
5 D. J. Tao, Z. M. Li, Z. Cheng, N. Hu and X. S. Chen, *Ind. Eng. Chem. Res.*, 2012, **51**, 16263–16269.
6 A. C. Cole, J. L. Jensen, I. Ntai, K. L. T. Tran, K. J. Weaver, D. C. Forbes and J. H. Davis, *J. Am. Chem. Soc.*, 2002, **124**, 5962–5963.
7 J. Z. Gui, X. H. Cong, D. Liu, X. T. Zhang, Z. D. Hu and Z. L. Sun, *Catal. Commun.*, 2004, **5**, 473–477.
8 H. Li, P. S. Bhadury, B. A. Song and S. Yang, *RSC Adv.*, 2012, **2**, 12525–12551.
9 C. P. Mehnert, R. A. Cook, N. C. Dispenziere and M. Afeworki, *J. Am. Chem. Soc.*, 2002, **124**, 12932–12933.
10 L. Zhang, Y. D. Cui, C. P. Zhang, L. Wang, H. Wan and G. F. Guan, *Ind. Eng. Chem. Res.*, 2012, **51**, 16590–16596.
11 N. Jiang, H. Jin, Y. H. Mo, E. A. Prasetyanto and S. E. Park, *Microporous Mesoporous Mater.*, 2011, **141**, 16–19.
12 L. Han, H. Q. Li, S. J. Choi, M. S. Park, S. M. Lee, Y. J. Kim and D. W. Park, *Appl. Catal., A*, 2012, **429**, 67–72.
13 B. Zhen, Q. Z. Jiao, Y. P. Zhang, Q. Wu and H. S. Li, *Appl. Catal., A*, 2012, **445**, 239–245.
14 Q. Zhang, H. Su, J. Luo and Y. Wei, *Green Chem.*, 2012, **14**, 201.
15 R. Sugimura, K. Qiao, D. Tomida and C. Yokoyama, *Catal. Commun.*, 2007, **8**, 770–772.
16 S. Doherty, J. G. Knight, J. R. Ellison, D. Weekes, R. W. Harrington, C. Hardacre and H. Manyar, *Green Chem.*, 2012, **14**, 925–929.
17 F. Liu, L. Wang, Q. Sun, L. Zhu, X. Meng and F. S. Xiao, *J. Am. Chem. Soc.*, 2012, **134**, 16948–16950.
18 C. DeCastro, E. Sauvage, M. H. Valkenberg and W. F. Holderich, *J. Catal.*, 2000, **196**, 86–94.
19 A. Zhu, T. Jiang, B. Han, J. Zhang, Y. Xie and X. Ma, *Green Chem.*, 2007, **9**, 169.
20 M. J. Jin, A. Taher, H. J. Kang, M. Choi and R. Ryoo, *Green Chem.*, 2009, **11**, 309–313.
21 B. W. Lu, T. Tsuda, H. Sasaki, Y. Oumi, K. Itabashi, T. Teranishi and T. Sano, *Chem. Mater.*, 2004, **16**, 286–291.
22 J. C. Groen, T. Sano, J. A. Moulijn and J. Perez-Ramirez, *J. Catal.*, 2007, **251**, 21–27.
23 R. Gounder and E. Iglesia, *Angew. Chem., Int. Ed.*, 2010, **49**, 808–811.
24 J. Miao, H. Wan, Y. Shao, G. Guan and B. Xu, *J. Mol. Catal. A: Chem.*, 2011, **348**, 77–82.
25 R. P. Singh, J. D. Way and S. F. Dec, *J. Membr. Sci.*, 2005, **259**, 34–46.
26 B. J. Campbell and A. K. Cheetham, *J. Phys. Chem. B*, 2002, **106**, 57–62.
27 H. H. Zhao, N. Y. Yu, Y. Ding, R. Tan, C. Liu, D. H. Yin, H. Y. Qiu and D. L. Yin, *Microporous Mesoporous Mater.*, 2010, **136**, 10–17.
28 J. M. Miao, H. Wan and G. F. Guan, *Catal. Commun.*, 2011, **12**, 353–356.
29 B. Zou, Y. Hu, L. Jiang, R. Jia and H. Huang, *Ind. Eng. Chem. Res.*, 2013, **52**, 2844–2851.

30 F. J. Liu, S. F. Zuo, W. P. Kong and C. Z. Qi, *Green Chem.*, 2012, **14**, 1342–1349.
31 L. Shao, Y. Du, G. Xing, W. Lv, X. Liang and C. Qi, *Monatsh. Chem.*, 2012, **143**, 1199–1203.
32 S. Wu, W. Dai, S. Yin, W. Li and C.-T. Au, *Catal. Lett.*, 2008, **124**, 127–132.
33 S. Gao, X. Liang, W. Cheng, W. Wang and J. Yang, *Chin. Sci. Bull.*, 2008, **53**, 1484–1488.
34 X. Liang, S. Gao, J. Yang, C. Liu, X. Yu and M. He, *Front. Chem. China*, 2007, **2**, 31–34.
35 S. M. Patel, U. V. Chudasama and P. A. Ganeshpure, *J. Mol. Catal. A: Chem.*, 2003, **194**, 267–271.